

Primordial black holes from Volkov–Akulov–Starobinsky supergravity

Yermek Aldabergenov ^{a,b,1} and Sergei V. Ketov ^{c,d,e,2}

^a *Department of Physics, Faculty of Science, Chulalongkorn University,
Phayathai Road, Pathumwan, Bangkok 10330, Thailand*

^b *Department of Theoretical and Nuclear Physics, Al-Farabi Kazakh National University,
71 Al-Farabi Ave., Almaty 050040, Kazakhstan*

^c *Department of Physics, Tokyo Metropolitan University
1-1 Minami-ohsawa, Hachioji-shi, Tokyo 192-0397, Japan*

^d *Research School of High-Energy Physics, Tomsk Polytechnic University
2a Lenin Avenue, Tomsk 634028, Russian Federation*

^e *Kavli Institute for the Physics and Mathematics of the Universe (WPI)
The University of Tokyo Institutes for Advanced Study, Kashiwa 277-8583, Japan*

Abstract

We study the formation of primordial black holes (PBH) in the Starobinsky supergravity coupled to the nilpotent superfield describing Volkov–Akulov goldstino. By using the no-scale Kähler potential and a polynomial superpotential, we find that under certain conditions our model can describe effectively single-field inflation with the ultra-slow-roll phase that appears near a critical (near-inflection) point of the scalar potential. This can lead to the formation of PBH as part of (or whole) dark matter, while keeping the inflationary spectral tilt and the tensor-to-scalar ratio in good agreement with the current cosmic microwave background (CMB) bounds. After inflation, supersymmetry is spontaneously broken at the inflationary scale with the vanishing cosmological constant.

¹yermek.a@chula.ac.th

²ketov@tmu.ac.jp

Contents

1	Introduction	2
2	Setup	3
2.1	Starobinsky inflation	4
2.2	Engineering a critical (near-inflection) point	6
3	Inflation and ultra-slow-roll	10
4	PBH and DM in our models	12
5	Conclusion	15
	Appendix: Mukhanov-Sasaki equation	16

1 Introduction

The nilpotent ($N = 1$) superfields can be used to describe the low-energy effective field theories with spontaneously broken and non-linearly realized supersymmetry (SUSY) [1–8] in four spacetime dimensions. The nilpotency condition $\mathbf{S}^2 = 0$ on a chiral superfield

$$\mathbf{S} = S + \sqrt{2}\theta\chi + \theta^2 F^S \tag{1}$$

has a solution

$$S = \frac{\chi^2}{2F^S}, \tag{2}$$

where S is the complex scalar, χ is the chiral fermion, and F^S is the complex auxiliary field. This solution is consistent only if $F^S \neq 0$. The χ can be identified with *goldstino* of the broken $N = 1$ SUSY. As regards inflationary dynamics, only scalar fields are relevant, hence, we can ignore the terms proportional to S or χ^2 in the scalar potential. The theory of a single nilpotent chiral superfield \mathbf{S} is known to be equivalent [1, 3, 7, 9] to the Volkov-Akulov (VA) theory [10].

Antoniadis, Dudas, Ferrara and Sagnotti proposed a Starobinsky-like model of inflation with the no-scale Kähler potential, coupled to the VA theory by using the nilpotent chiral superfield, which was dubbed the Volkov-Akulov-Starobinsky (VAS) supergravity [11]. During inflation, the VAS model [11] is consistent with the nilpotency constraint because $F^S \neq 0$. However, the F^S vanishes in a Minkowski vacuum, which makes the solution $S = \chi^2/(2F^S)$ singular. The improved and generalized version of the VAS model with a non-vanishing F^S in vacuum also, was proposed in Ref. [12] with the same no-scale Kähler potential. The alternative VAS model with consistent vacuum structure but a different Kähler potential was studied in Ref. [13].

On the other hand, primordial black holes (PBH) is an interesting area of research that can give us more information about the inflationary and post-inflationary epoch. The absence of PBH signals in cosmological and astrophysical observations can constrain our models, whereas, if found, PBH masses and their distribution could teach us important details about the mechanisms of PBH production. There is also an intriguing possibility that PBH of certain masses make up the observed dark matter (DM), see e.g., Refs. [14, 15] for a review.

In this paper we consider PBH (as part of or whole DM) from the VAS supergravity.¹ We generalize the model of Ref. [12] by extending the polynomial superpotential in order to derive the necessary conditions for the PBH production after inflation, and estimate PBH masses and abundance for the present DM. We employ the standard scenario of PBH formation from single-field models of inflation, based on engineering a near-inflection point in the inflaton scalar potential leading to the ultra-slow-roll phase of inflation and the enhancement (peak) in the power spectrum of scalar curvature perturbations [24, 25]. Then the emerging large perturbations gravitationally collapse into PBH. We do not address non-Gaussianities and loop corrections in this paper, see Refs. [26–28] for their possible impact.

Our paper is organized as follows. Sec. 2 is our setup, where we recover the original Starobinsky model, and demonstrate how to create a stationary near-inflection point for the ultra-slow-roll (USR) phase. In Sec. 3 we numerically derive inflationary solutions and show viability of our new model. The main part is Sec. 4 devoted to PBH formation from enhanced scalar perturbations and the related PBH-DM scenario. We also find the scalar-induced gravitational waves (GW) spectrum that can be tested by future space-based GW experiments. In Appendix we briefly summarize the technical details related to Mukhanov-Sasaki (MS) equation. We set the reduced Planck mass $M_{\text{Pl}} = 1$ unless it is stated otherwise.

2 Setup

The original VAS supergravity model [11] uses the no-scale Kähler potential for the inflaton chiral superfield T and the nilpotent superfield S as

$$K = -3 \log(T + \bar{T} - S\bar{S}) , \quad (3)$$

with the superpotential

$$W = S(b_0 + b_1 T) , \quad (4)$$

having constant parameters b_0 and b_1 . Since $S^2 = 0$, both K and W are linear with respect to S and \bar{S} . Though this model does describe SUSY breaking during inflation, SUSY is restored in a Minkowski minimum, leading to $F^S = 0$ that is inconsistent with the solution (2). The VAS model [11] was improved in Ref. [12] by extending the superpotential to

$$W = A[a_0 + a_1 T + S(b_0 + b_1 T)] \quad (5)$$

under certain conditions on the parameters to get a non-vanishing vacuum expectation value (VEV) $\langle F^S \rangle$. The parameter A can be used to rescale one of the non-vanishing parameters a or b to unity. All the parameters of the superpotential (5) are chosen to be real.

Our aim is to study further extensions of the superpotential (5) toward PBH production in the VAS framework by adding an ultra-slow-roll (USR) regime in the effective single-field inflation scenario that requires the scalar potential to have a critical (near-inflection) point [24, 29]. The Kähler potential (3) will be unchanged.

Let us consider a more general superpotential

$$W = A[f(T) + Sg(T)] , \quad (6)$$

¹As regards PBH formation in other Starobinsky-like supergravity-based inflationary models like the α -attractors, see e.g., Refs. [16–23].

where $f(T)$ and $g(T)$ are polynomials in T . The F-type scalar potential is given by

$$V_F = e^K \left[K^{I\bar{J}} D_I W D_{\bar{J}} \bar{W} - 3W\bar{W} \right] , \quad (7)$$

where $K^{I\bar{J}}$ is the inverse Kähler metric, the indices I, J run over the chiral superfields, and $D_I W = W_I + K_I W$, with the subscripts denoting the derivatives. The auxiliary F -fields are given by

$$F^I = -e^{K/2} K^{I\bar{J}} D_{\bar{J}} \bar{W} . \quad (8)$$

In our model with the single chiral nilpotent superfield S , the Kähler metric becomes diagonal after using the constraint $S^2 = 0$ and ignoring the fermions, with $K_S = 0$. This implies that $F^S \propto \bar{W}_{\bar{S}} \neq 0$ for the consistency of the solution with the constraint. We also introduce the Kähler-invariant F -fields as

$$|F^S| \equiv \sqrt{K_{S\bar{S}} F^S \bar{F}^{\bar{S}}} , \quad |F^T| \equiv \sqrt{K_{T\bar{T}} F^T \bar{F}^{\bar{T}}} . \quad (9)$$

2.1 Starobinsky inflation

There are several ways to realize Starobinsky inflation [30] in supergravity, as well as in our models, see e.g., Ref. [20] for a review and Ref. [31] for possible extensions. Here we use the no-scale Kähler potential (3) and the superpotential

$$W = A[a_0 + a_1 T + a_2 T^2 + a_3 T^3 + S(b_0 + b_1 T + b_2 T^2)] , \quad (10)$$

where we have expanded the functions $f(T)$ and $g(T)$ of Eq. (6) in Taylor series up to the cubic and quadratic terms, respectively. Equation (10) leads to the scalar potential $V = V_F$ given by

$$\begin{aligned} \frac{12}{A^2} V &= (b_0^2 - 6a_0 a_1) \phi^{-2} + 2(b_0 b_1 - 2a_1^2 - 6a_0 a_2) \phi^{-1} \\ &+ (b_1^2 + 2b_0 b_2 - 10a_1 a_2 - 18a_0 a_3) + 2(b_1 b_2 - 2a_2^2 - 6a_1 a_3) \phi + (b_2^2 - 6a_2 a_3) \phi^2 , \end{aligned} \quad (11)$$

where we have used the parametrization

$$T = \phi + i\tau , \quad (12)$$

and have set the axion/sinflaton $\tau = 0$ by assuming it to be stabilized, as will be shown below.

The canonical parametrization of the inflaton is given by ²

$$\phi = \langle \phi \rangle \exp \left(-\sqrt{2/3} \varphi \right) , \quad (13)$$

so that ϕ is always positive, while in vacuum we always have $\varphi = 0$. By looking at Eq. (11), it can be seen that there are two ways to obtain a Starobinsky-like plateau, i.e. a nearly-flat inflaton potential. One way is to keep only negative powers of ϕ (and a constant term) by eliminating the positive powers, which can be done by the appropriate choice of the parameters. In this case the potential asymptotically approaches a constant value at $\varphi \rightarrow -\infty$. Another way is to keep only positive powers of ϕ , so that the potential approaches a constant at $\varphi \rightarrow +\infty$. We get the conditions on the parameters for both ways, and explain why we choose the second way to study PBH formation below.

²The sign in front of φ is arbitrary, and we choose the negative sign.

Inflation for negative φ . Starobinsky-like inflation for large negative φ (i.e. large values of ϕ) can be obtained from the potential (11) by arranging the coefficients at ϕ and ϕ^2 to be zero. For example, this can be done by setting $a_2 = b_2 = 0$, and either $a_1 = 0$ or $a_3 = 0$ (in Ref. [12], only the case of $a_2 = b_2 = a_3 = 0$ was considered). The higher-order terms (a_4, a_5, b_3, b_4 , etc.) are prohibited because they would lead to positive powers of ϕ in the scalar potential, which can unflatten the inflationary plateau unless the corresponding parameters are extremely small. These restrictions on the parameters make it difficult to create an inflection point in the potential in order to realize USR inflation, and subsequently PBH production. Therefore, we consider the alternative scenario where inflation takes place for large positive φ or small ϕ .³

Inflation for positive φ . In this case we keep only positive powers of ϕ in Eq. (11), so that the potential approaches a constant value at $\varphi \rightarrow +\infty$, which corresponds to $\phi \rightarrow 0$. This can be done by setting $a_1 = b_0 = 0$, and either (I) $a_0 = 0$ or (II) $a_2 = 0$ (or both). In the first case, $a_1 = b_0 = a_0 = 0$, the scalar potential reads

$$\frac{12}{A^2}V = b_1^2 + 2(b_1b_2 - 2a_2^2)\phi + (b_2^2 - 6a_2a_3)\phi^2. \quad (14)$$

We can further simplify the model by setting either $b_2 = 0$ (model I-a) or $a_3 = 0$ (model I-b). In the former case, the Minkowski vacuum equations $V = 0$ and $\partial_\phi V \equiv V_\phi = 0$ yield

$$a_3 = -\frac{2a_2^3}{3b_1^2}, \quad \langle\phi\rangle = \frac{b_1^2}{2a_2^2}. \quad (15)$$

Without loss of generality we can set $a_2 = 1$ (by rescaling A and other parameters), which also leads to $a_3 < 0$. By using the canonical parametrization $\phi = \langle\phi\rangle e^{-\sqrt{2/3}\varphi} = b_1^2 e^{-\sqrt{2/3}\varphi}/2$, we get the Starobinsky potential

$$V = \frac{A^2 b_1^2}{12} \left(1 - e^{-\sqrt{\frac{2}{3}}\varphi}\right)^2. \quad (16)$$

As was already mentioned above, consistency of our construction requires $D_S W = W_S \neq 0$ over the whole inflationary history, which is satisfied both during and after inflation for the parameter choice I. In particular, in the Minkowski vacuum we get $\langle W_S \rangle = -Ab_1^3/2$, while the Kähler-invariant F-terms are given by

$$\langle |F^S| \rangle = \langle |F^T| \rangle = \frac{Ab_1}{2\sqrt{3}}. \quad (17)$$

We also find that the axion τ is stabilized with the vanishing VEV in the Minkowski vacuum and the positive mass squared, $m_\tau^2 = A^2 b_1^2/9$ (after canonical rescaling), that can be chosen beyond the Hubble scale during inflation. The effective axion mass at the horizon exit can be roughly estimated in the limit $e^{-\sqrt{2/3}\varphi} \rightarrow 0$, which yields $m_{\tau,\text{eff.}} \simeq m_\tau$, i.e. it is near the axion mass in the vacuum.

Another route to the Starobinsky potential (model I) is given by the case I-b, where $a_3 = 0$ and $b_2 \neq 0$. The vacuum equations for the potential (14) imply

$$b_2 = \frac{a_2^2}{b_1}, \quad \langle\phi\rangle = \frac{b_1^2}{a_2^2}, \quad (18)$$

³Inflation in our models is always of the single-large-field-type in terms of the canonical inflaton φ .

while we can set $a_2 = 1$ by rescaling the parameter A . In terms of the canonical inflaton $\phi = \langle \phi \rangle e^{-\sqrt{2/3}\varphi}$, we obtain the same Starobinsky potential (16). In this case, the axion mass is unchanged, $m_\tau^2 = A^2 b_1^2/9$, being also approximately equal to the effective mass during early inflation. SUSY is broken by the F-field VEV, which are slightly different from the I-a case,

$$\langle |F^S| \rangle = \frac{1}{\sqrt{3}} A b_1, \quad \langle |F^T| \rangle = \sqrt{\frac{2}{3}} A b_1. \quad (19)$$

The model II uses $a_1 = b_0 = a_2 = 0$. It leads to the scalar potential

$$\frac{12}{A^2} V = b_1^2 - 18 a_0 a_3 + 2 b_1 b_2 \phi + b_2^2 \phi^2, \quad (20)$$

whose stationary point equation is solved by $b_1 + b_2 \phi = 0$. This is, however, problematic because the F-field of the nilpotent superfield,

$$F^S \propto \bar{W}_{\bar{S}} = \bar{T}(b_1 + b_2 \bar{T}) = \phi(b_1 + b_2 \phi), \quad (21)$$

vanishes at the stationary point (the minimum) when the axion τ vanishes, which is inconsistent with the solution to the nilpotency constraint. Therefore, model II is excluded from our discussion.

Elimination of irrelevant parameters. Given the polynomial superpotential in the form (6), two of its *non-vanishing* parameters can be eliminated by reparametrisation. Let us rewrite the superpotential as

$$W = A \sum_{i=m} a_i T^i + A S \sum_{j=n} b_j T^j, \quad (22)$$

where the integers m and n are positive, and the summation upper limits are arbitrary but greater than the lower limits. We assume that the lowest-order parameters a_m and b_n are non-vanishing. The coefficient a_m (or any one of the non-vanishing a_i -coefficients) can always be set to unity by rescaling A and the other parameters accordingly, while b_n can be eliminated by the following redefinitions of the fields and the parameters:

$$\begin{aligned} T &\rightarrow T b_n^k, & S &\rightarrow S b_n^{k/2}, \\ a_i &\rightarrow a_i b_n^{k(m-i)}, & b_j &\rightarrow b_j b_n^{k(m-j-1/2)}, \\ A &\rightarrow A b_n^{-km}, & k &\equiv (m - n - \frac{1}{2})^{-1}, \end{aligned} \quad (23)$$

for $i > m$ and $j > n$. The superpotential (22) is invariant under the transformation (23), while the Kähler potential $K = -3 \log(T + \bar{T} - S\bar{S})$ is shifted by an irrelevant constant,

$$K \rightarrow K - 3 \log b_n^k, \quad (24)$$

which can be absorbed by rescaling W . Therefore, we fix the lowest-order non-vanishing parameters as $a_m = b_n = 1$ without loss of generality in what follows.

2.2 Engineering a critical (near-inflection) point

To accommodate a near-inflection point, in general, the potential must be at least cubic in ϕ . However, due to the non-trivial structure of the scalar potential in supergravity, the higher-order terms may be also needed. We find that it is sufficient to add a quartic term to the

superpotential, either $W \supset Aa_4T^4$ or $W \supset Ab_3ST^3$. We demonstrate that the ultimate superpotential must have the form ⁴

$$W = A[a_0 + T^2 + a_3T^3 + S(T + b_2T^2)] + \Delta W , \quad (25)$$

where ΔW should be either Aa_4T^4 or Ab_3ST^3 (we consider both cases below), while the a_0 -term is needed to obtain the observed value of the spectral tilt n_s (within 1σ CL).

Model with $\Delta W = Aa_4T^4$. In this case we begin with the minimal superpotential that allows an inflection point,

$$W = A(T^2 + a_3T^3 + a_4T^4 + ST) , \quad (26)$$

where we have $a_0 = b_2 = 0$ at first, and further explain why $b_2 \neq 0$ is needed. The impact of the parameter a_0 is studied in Sec. 3. In Eq. (26) we have two free parameters (a_3 and a_4) to create an inflection point. We also set a Minkowski minimum after inflation. The parameter A is responsible for the height of the inflationary plateau and, therefore, the scale of inflation. The choice (26) leads to

$$\frac{12}{A^2}V = 1 - 4\phi - 6a_3\phi^2 - 4a_4\phi^3 + 6a_3a_4\phi^4 + 8a_4^2\phi^5 . \quad (27)$$

The stationary point equation can be conveniently written as

$$\frac{3}{A^2}V_\phi = Z_1Z_2 = 0 ; \quad Z_1 \equiv -1 + 2a_4\phi^2 , \quad Z_2 \equiv 1 + 3a_3\phi + 5a_4\phi^2 , \quad (28)$$

so that its four stationary points are the solutions to two quadratic equations $Z_1 = 0$ and $Z_2 = 0$. A stationary inflection point, which we call $\tilde{\phi}$, must satisfy the equations $V_\phi = V_{\phi\phi} = 0$, which also fixes one of the parameters. Another parameter, along with $\langle\phi\rangle$, can be fixed by the Minkowski vacuum equations $V = V_\phi = 0$. We want a near-inflection point to be between the horizon exit $\phi_* \approx 0$ and the vacuum $\langle\phi\rangle$, so we search for solutions to the two sets of equations satisfying this condition. We find the desired inflection point solves $Z_2 = 0$, and it is given by $\tilde{\phi} = -2/(3a_3)$ with the parameter $a_4 = 9a_3^2/20$ fixed by the equation $V_{\phi\phi} = 0$. This implies that $a_3 < 0$ and $a_4 > 0$. Subsequently, using the Minkowski vacuum equations, we find

$$a_3 = \frac{10 - 4\sqrt{10}}{3} , \quad \langle\phi\rangle = -\frac{\sqrt{10}}{3a_3} , \quad (29)$$

where $\langle\phi\rangle$ solves $Z_1 = 0$. The scalar potential (27) with the canonical inflaton $\phi = \langle\phi\rangle e^{-\sqrt{2/3}\varphi}$ and the fixed a_3 and a_4 as above, reads

$$\frac{12}{A^2}V = \frac{2\sqrt{10} - 5 - 2\sqrt{10}x + 10x^2 - \sqrt{10}x^3 - 5x^4 + \sqrt{10}x^5}{2\sqrt{10} - 5} , \quad x \equiv e^{-\sqrt{2/3}\varphi} . \quad (30)$$

Its plot is shown in Fig. 1. The fact that there are no free parameters left in Eq. (30) means that we can tune the shape of the potential in the vicinity of the inflection point (by tuning a_4) but the height of the inflection point (against the slow-roll plateau) cannot be controlled.

Our numerical analysis of the equations of motion shows that it is difficult to obtain an USR regime near the inflection point because of its shallow nature and the lack of control over

⁴Here, for convenience, we choose $a_2 = 1$ (and not $a_0 = 1$) because a_0 must be very small compared to the other parameters that are of the order one, as is explained below.

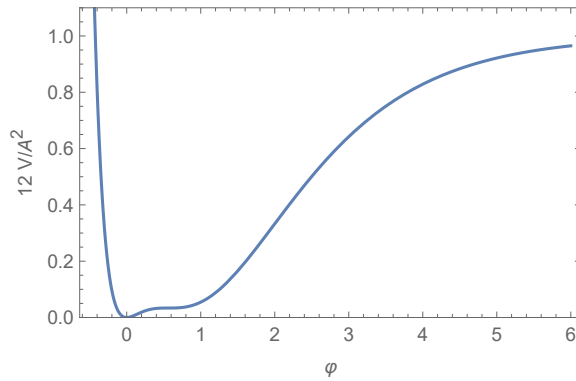


Figure 1: The scalar potential (30) in the "minimal" model with a near-inflection point. The inflection point is shallow and cannot be raised in this model.

the potential. However, the situation can be improved by turning on another parameter. We find that it is enough to turn on b_2 . It extends the previous "minimal" superpotential and the resulting scalar potential as follows:

$$W = A[T^2 + a_3T^3 + a_4T^4 + S(T + b_2T^2)] , \quad (31)$$

$$\frac{12}{A^2}V = 1 + 2(b_2 - 2)\phi + (b_2^2 - 6a_3)\phi^2 - 4a_4\phi^3 + 6a_3a_4\phi^4 + 8a_4^2\phi^5 . \quad (32)$$

Given the non-vanishing b_2 parameter, the stationary equation $V_\phi = 0$ loses its simple factorized form (28) and becomes a more general quartic polynomial equation for its roots. However, we can get an approximate analytical solution by using our previous result, when $|b_2| \ll 1$. This is helpful to qualitatively study the behavior of the potential with increasing $|b_2|$. For small $|b_2|$, we Taylor-expand $\tilde{\phi}$, $\langle\phi\rangle$, a_4 , and a_3 as

$$\begin{aligned} \tilde{\phi} &= \tilde{\phi}_0 + \tilde{\phi}_1 b_2 + \mathcal{O}(b_2^2) , \\ \langle\phi\rangle &= \langle\phi\rangle_0 + \langle\phi\rangle_1 b_2 + \mathcal{O}(b_2^2) , \\ a_4 &= a_{4(0)} + a_{4(1)} b_2 + \mathcal{O}(b_2^2) , \\ a_3 &= a_{3(0)} + a_{3(1)} b_2 + \mathcal{O}(b_2^2) , \end{aligned} \quad (33)$$

where $\tilde{\phi}_0$, $\langle\phi\rangle_0$, $a_{4(0)}$, and $a_{3(0)}$ are given by the "unperturbed" ($b_2 = 0$) solutions for the potential (27),

$$\tilde{\phi}_0 = -\frac{2}{3a_{3(0)}} , \quad \langle\phi\rangle_0 = -\frac{\sqrt{10}}{3a_{3(0)}} , \quad a_{4(0)} = \frac{9a_{3(0)}^2}{20} , \quad a_{3(0)} = \frac{10 - 4\sqrt{10}}{3} . \quad (34)$$

Solving the equations in the subleading order with respect to b_2 yields

$$\begin{aligned} \tilde{\phi}_1 &= \frac{18a_{3(1)} + 5a_{3(0)}}{27a_{3(0)}^2} , \quad \langle\phi\rangle_1 = \frac{16 + \sqrt{10}}{216} , \\ a_{4(1)} &= \frac{3a_{3(0)}}{40}(12a_{3(1)} + 5a_{3(0)}) , \quad a_{3(1)} = \frac{11\sqrt{10} - 25}{9} . \end{aligned} \quad (35)$$

To get a dependence of the height of the inflection point upon small variations of b_2 , we calculate the ratio $V(\tilde{\phi})/V(0)$, i.e. the ratio of the value of V at the inflection point to its asymptotic value at the slow-roll plateau where $\phi \simeq 0$. We find

$$\frac{V(\tilde{\phi})}{V(0)} \approx 0.03 - 0.28b_2 + \mathcal{O}(b_2^2) . \quad (36)$$

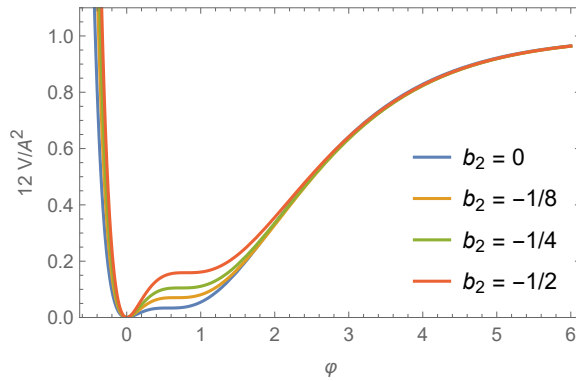


Figure 2: The scalar potential (32) (in the model a_4) for some values of b_2 . The a_3 and a_4 are derived from the inflection point and vacuum equations, while their values are collected in Table 1.

Hence, in order to raise the height of the inflection point, we need $b_2 < 0$. We confirm that by choosing a small negative b_2 and numerically solving the inflection point (and the Minkowski vacuum) equations. This leads to the scalar potential shown in Fig. 2, where we set $b_1 = 1$ and choose different values of b_2 . The corresponding parameter sets are shown in Table 1.

b_2	0	-1/8	-1/4	-1/2
a_3	-0.8830	-1.0271	-1.1831	-1.5166
a_4	0.3509	0.4326	0.5320	0.7753

Table 1: The parameter sets used in Fig. 2 for the model with the scalar potential (32).

The model $\Delta W = Ab_3ST^3$. In this model we have

$$W = A[T^2 + a_3T^3 + S(T + b_2T^2 + b_3T^3)] , \quad (37)$$

where we use the non-vanishing b_2 -parameter, as is required by the inflection point and the Minkowski vacuum conditions. This leads to the following scalar potential:

$$\frac{12}{A^2}V = 1 + 2(b_2 - 2)\phi + (b_2^2 - 6a_3 + 2b_3)\phi^2 + 2b_2b_3\phi^3 + b_3^2\phi^4 . \quad (38)$$

In this case, the inflection point and the vacuum are hard to find analytically, so we solve the equations numerically, by varying b_2 as a free parameter, and fixing a_3 and b_3 by the stationary points determined by the vacuum and inflection point equations. We find that the inflection point exists for b_2 slightly larger than one, as is shown in Fig. 3. The corresponding parameter sets are collected in Table 2.

b_2	1.01	1.03	1.05	1.07
a_3	-0.1575	-0.1559	-0.1576	-0.1606
b_3	-0.2399	-0.2442	-0.2533	-0.2647

Table 2: The parameter sets used in Fig. 3 for the model with the scalar potential (38).

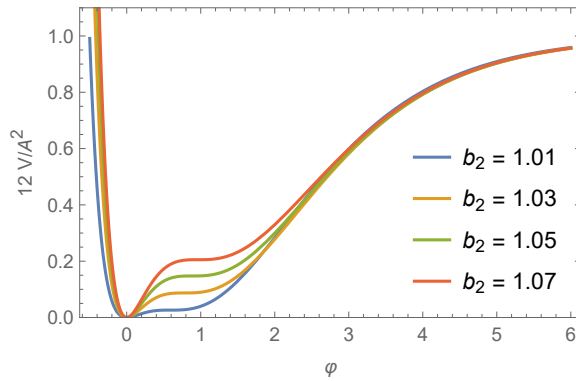


Figure 3: The scalar potential (38) in the model b_3 with b_2 around unity. The values of a_3 and b_3 are shown in Table 2. When $b_2 \leq 1$, the inflection point vanishes.

3 Inflation and ultra-slow-roll

In this Section we demonstrate viable inflation with a short USR period in our near-inflection-point models of supergravity. We begin with the model a_4 defined by Eqs. (31) and (32), and Fig. 2, where we fix $b_2 = -1/2$. We denote the duration of the first (SR) and second (USR) inflationary stages as ΔN_1 and ΔN_2 , respectively, and set the total inflation duration as $\Delta N_1 + \Delta N_2 = 55$, by assuming the CMB reference scale $k = 0.05 \text{ Mpc}^{-1}$ leaving the horizon 55 e-folds before the end of inflation.

For this purpose, we fix $\Delta N_2 = 20$ by adjusting the parameter a_3 around its inflection point value, while a_4 is to be fixed by the Minkowski vacuum equations. The desired outcome is obtained for

$$a_3 = -1.5157647, \quad a_4 = 0.774006, \quad (39)$$

and the corresponding inflationary solution is shown in Fig. 4, which includes the inflaton evolution $\varphi(N)$, the Hubble function $H(N)$, and the Hubble slow-roll parameters

$$\epsilon \equiv -\frac{H'}{H}, \quad \eta \equiv \frac{\epsilon'}{\epsilon}, \quad (40)$$

during the last 55 e-folds. The primes denote the derivatives with respect to N . The end of the first stage is defined by the local maximum of ϵ because it does not reach one at that time. The end of the second stage is defined by $\epsilon = 1$. The initial conditions are set to $\varphi(0) = 6.5$ and $\varphi'(0) = 0.01$.

As is clear from Fig. 4, the ϵ significantly dips during USR, as may be expected from the presence of a near-inflection point in the potential. This leads to a large enhancement in the scalar power spectrum. Before computing the power spectrum, we derive the inflationary observables (cosmological tilts) n_s and r at the horizon exit (with 55 e-folds before the end of inflation), by using the standard formulae

$$n_s = 1 - 2\epsilon - \eta, \quad r = 16\epsilon. \quad (41)$$

For the model and the parameters under consideration, we find

$$n_s = 0.9430, \quad r = 0.0093. \quad (42)$$

Therefore, the spectral tilt n_s is outside the 3σ CMB limits [32,33]. This problem can be solved by turning on one of the subleading parameters in the superpotential. In the Starobinsky

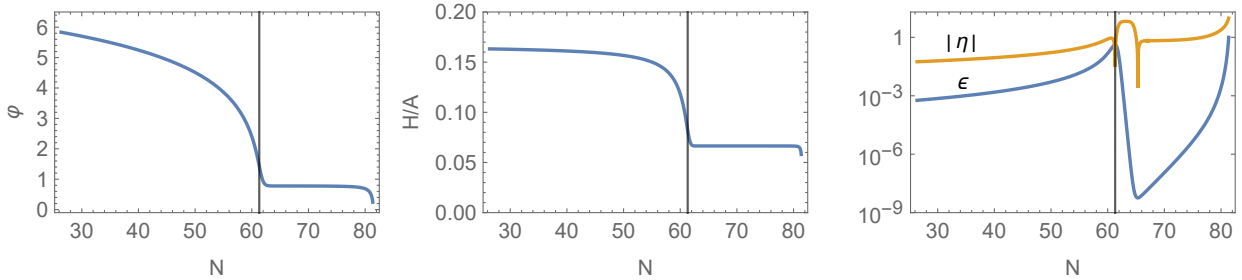


Figure 4: The numerical solutions to the equations of motion in terms of $\varphi(N)$ (on the left), $H(N)$ (in the center), and slow-roll parameters (on the right). The last 55 e-folds are shown. The vertical line represents transition from SR to USR. The duration of the USR stage is fixed to $\Delta N_2 = 20$.

inflation model, the horizon exit happens in a relatively flat region of the scalar potential. However, if we introduce an USR regime near the inflection point, it will shift the horizon exit towards the minimum of the potential, thus reducing the value of n_s . This can be counteracted by introducing a term in the scalar potential which grows with φ , and flattens the potential in the region where the horizon exit happens. When looking at the scalar potential (11) originating from the subleading terms in the superpotential, we find that the ϕ^{-1} -term is suitable for this purpose because it is proportional to $e^{\sqrt{2/3}\varphi}$. For example, this term can be turned on by using a negative a_0 parameter that must be tuned in order to keep the potential flat near the horizon exit. To summarize, we get the superpotential and the scalar potential (for the a_4 model) with the inclusion of a_0 as follows:

$$W = A[a_0 + T^2 + a_3 T^3 + a_4 T^4 + S(T + b_2 T^2)] , \quad (43)$$

$$V/A^2 = -a_0 \phi^{-1} + \frac{1}{2} \left(\frac{1}{6} - 3a_0 a_3 \right) - \frac{1}{6} (2 + 12a_0 a_4 - b_2) \phi - \frac{1}{12} (6a_3 - b_2^2) \phi^2 - \frac{1}{3} a_4 \phi^3 + \frac{1}{2} a_3 a_4 \phi^4 + \frac{2}{3} a_4^2 \phi^5 . \quad (44)$$

The value of a_0 can be chosen to raise n_s , the a_3 controls the shape of the potential near the inflection point, the a_4 is fixed by the Minkowski vacuum equations, and the b_2 controls the height of the inflection point. As for the power spectrum enhancement in the single-field near-inflection-point models, it depends on both the height of the inflection point, and the shape of the potential near it. Therefore, it is a combination of a_3 and b_2 that controls the power spectrum peak, which we also confirm numerically. The power spectrum of scalar perturbations is derived in the next Section.

Figure 5 shows how small negative values of a_0 change the scalar potential at large φ defined by $\phi = \langle \phi \rangle e^{-\sqrt{2/3}\varphi}$. The parameters a_3 and a_4 are fixed in Table 3 by demanding $\Delta N_2 = 20$ and a Minkowski vacuum. Small changes between the three sets of parameters are due to the small variations in a_0 . The evolution of φ , H , ϵ , and η in the three cases is nearly the same as in Fig. 4.⁵ Table 3 shows the values of n_s and r for the given parameter sets. When $a_0 = -7 \times 10^{-6}$, the spectral tilt n_s is already within 1σ CMB limits, which is the significant improvement compared to $a_0 = 0$ case. As for the tensor-to-scalar ratio r , it tends to larger values with increasing a_0 , though still within the current CMB bounds [32, 33]. Here we used the duration $\Delta N_2 = 20$ of the USR as an example. In the next Section we give the specific

⁵Though adding a small value to a_0 modifies the Starobinsky-like inflationary plateau for large φ , we find no noticeable increase in the dependence of the inflationary solutions upon initial conditions.

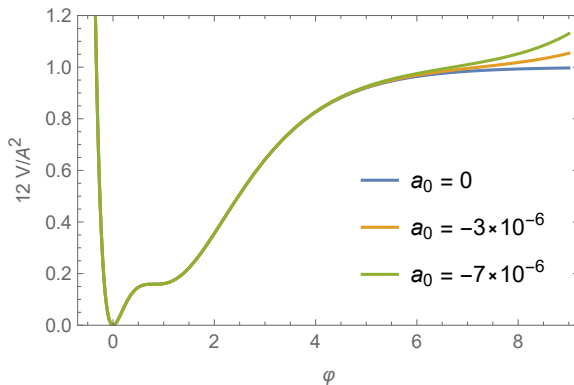


Figure 5: The scalar potential (44) after turning on a_0 . The $b_2 = -1/2$, the a_3 and a_4 are given in Table 3. The CMB scales leave the horizon when $\phi \approx 6$, as can be seen from Fig. 4. The evolution of φ , H and SR parameters is nearly the same for all three choices of a_0 .

values of the parameters in order to obtain PBH with the masses of $10^{18} - 10^{22}$ g, suitable for the whole DM, where slightly larger values of ΔN_2 are favored in both (a_4 and b_3) models.

We find that the b_3 model of Eq. (37) leads to nearly the same results for the inflationary dynamics and observables, like the a_4 model. In particular, adding a small negative a_0 -parameter to the b_3 model helps to raise the value of n_s when ΔN_2 is around 20.

a_0	a_3	a_4	b_2	n_s	r
0	-1.5157647	0.774006	-1/2	0.9430	0.0093
-3×10^{-6}	-1.5157049	0.773923	-1/2	0.9507	0.0107
-7×10^{-6}	-1.5156251	0.773813	-1/2	0.9614	0.0129

Table 3: The parameter sets for three different values of a_0 , showing the impact of a small negative a_0 on the spectral tilt n_s and the tensor-to-scalar ratio r . The a_3 and a_4 are tuned to obtain the USR duration $\Delta N_2 = 20$ in all three cases.

4 PBH and DM in our models

Assuming PBH formation during the radiation era, we use the Press-Schechter formalism [34] to estimate the PBH mass function from a given power spectrum. We use the following expressions for the PBH mass, the PBH production rate, and the density contrast [35, 36]:

$$M_{\text{PBH}}(k) \simeq 10^{20} \left(\frac{7 \times 10^{12}}{k \text{ Mpc}} \right)^2 \text{ g}, \quad \beta_f(k) \simeq \frac{\sigma(k)}{\sqrt{2\pi}\delta_c} e^{-\frac{\delta_c^2}{2\sigma^2(k)}}, \quad (45)$$

$$\sigma^2(k) = \frac{16}{81} \int \frac{dq}{q} \left(\frac{q}{k} \right)^4 e^{-q^2/k^2} P_{\mathcal{R}}(q), \quad (46)$$

where δ_c is the density threshold (critical density) for PBH formation. It was estimated as $\delta_c \simeq 1/3$ [37], but numerical analysis gives larger values $0.41 \lesssim \delta_c \lesssim 2/3$ [38]. In our calculations we choose the reference value $\delta_c = 0.45$. Then the PBH fraction can be estimated as

$$\frac{\Omega_{\text{PBH}}(k)}{\Omega_{\text{DM}}} \equiv f(k) \simeq \frac{1.2 \times 10^{24} \beta_f(k)}{\sqrt{M_{\text{PBH}}(k) \text{g}^{-1}}}. \quad (47)$$

The numerical factor 1.2 was obtained by assuming the Minimal Supersymmetric Standard Model (MSSM) physical degrees of freedom (for the Standard Model it becomes 1.4). The total PBH-to-DM fraction reads

$$f_{\text{tot}} = \int d(\log M_{\text{PBH}}) f(M_{\text{PBH}}) . \quad (48)$$

In order to derive the PBH mass function from the equations above, we have to get the power spectrum of scalar perturbations. We do this numerically by solving the Mukhanov-Sasaki (MS) equation [39, 40] given in Appendix.

First, we consider the a_4 model defined by the superpotential (43) including the a_0 parameter, and find the parameter choice giving rise to $f_{\text{tot}} = 1$, i.e. the PBH as the whole DM, while keeping the acceptable values of n_s and r ,⁶

$$a_0 = -1.4 \times 10^{-5} , \quad a_3 = -1.487732305 , \quad a_4 = 0.75173 , \quad b_2 = -0.48 . \quad (49)$$

This example leads to the duration of the USR stage $\Delta N_2 = 25.53$, and the inflationary observables

$$n_s = 0.9636 , \quad r = 0.0208 . \quad (50)$$

The corresponding numerical plots are shown in Fig. 6, including the scalar potential (top-left), the Hubble function (top-right), the slow-roll parameters (bottom-left), and the power spectrum (bottom-right). The latter shows a large enhancement (slightly exceeding $P_{\mathcal{R}} = 10^{-2}$) in the power spectrum near the scale $k = 10^{13} \text{ Mpc}^{-1}$. We use this power spectrum in Eq. (46) to calculate the density contrast and eventually the PBH mass function (47), which is shown in Fig. 7 as the solid black curve. The PBH fraction peaks near 10^{19} g .

Similar results with the PBH-DM scenario are obtained from the b_3 model as well. We extend the model in Eq. (37) by adding the a_0 -term as

$$W = A[a_0 + T^2 + a_3 T^3 + S(T + b_2 T^2 + b_3 T^3)] , \quad (51)$$

$$\begin{aligned} V/A^2 = & -a_0 \phi^{-1} + \frac{1}{2} \left(\frac{1}{6} - 3a_0 a_3 \right) - \frac{1}{6} (2 - b_2) \phi \\ & - \frac{1}{12} (6a_3 - b_2^2 - 2b_3) \phi^2 + \frac{1}{6} b_2 b_3 \phi^3 + \frac{1}{12} b_3^2 \phi^4 . \end{aligned} \quad (52)$$

To realize the whole PBH-DM scenario, we take the following parameters:

$$a_0 = -3.7 \times 10^{-5} , \quad a_3 = -0.1566928828 , \quad b_2 = 1.044 , \quad b_3 = -0.249931 , \quad (53)$$

which lead to the inflationary (CMB) predictions

$$n_s = 0.9616 , \quad r = 0.0216 , \quad (54)$$

and the PBH mass function given by the dashed curve in Fig. 7, where the peak is located near 10^{20} g . The USR stage lasts for $\Delta N_2 = 25.94$ e-folds. We do not show plots of the inflationary solution in this case because they are nearly identical to Fig. 6, including the shape of the power spectrum.

The low-mass PBH-DM formation is known to produce the notable stochastic GW background induced by enhanced scalar perturbations, within the frequencies of the planned space-based detectors such as LISA [42] and DECIGO [43]. To calculate this GW background, we use the formalism of Refs. [44, 45], see also Section 7 of Ref. [21]. The resulting GW density is shown in Fig. 8. The induced primordial GW signal caused by scalaron would be a clear

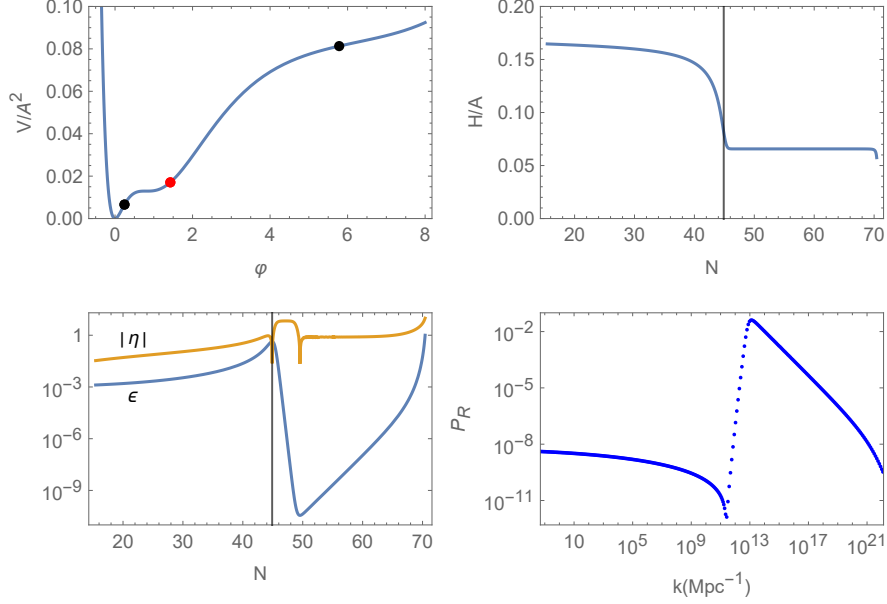


Figure 6: The inflationary solution in the a_4 model with the parameter choice (49). The top-left plot is the scalar potential with the black dots representing the start and the end of the last 55 e-folds, and the red dot showing the end of the first (slow-roll) stage. The top-right and bottom-left plots show the Hubble function and the slow-roll parameters, respectively (the vertical lines show the end of the first stage). The bottom-right plot is the power spectrum of scalar perturbations, where the large peak is near the scale 10^{13}Mpc^{-1} .

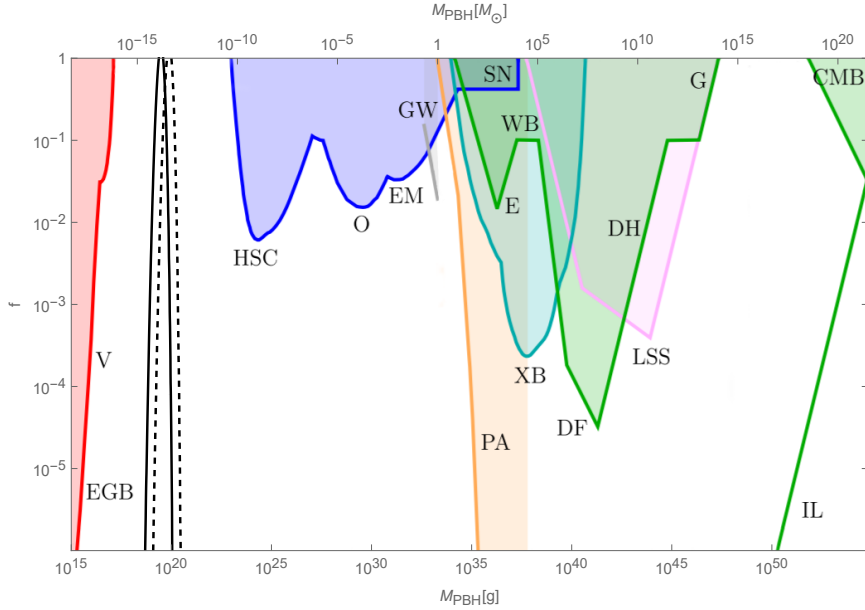


Figure 7: The PBH-to-DM mass function in the a_4 model with the parameters (49) (the solid black curve), and in the b_3 model with the parameters (53) (the dashed curve). In both cases, $f_{\text{tot}} = 1$. The background of observational constraints is taken from Refs. [15, 41].

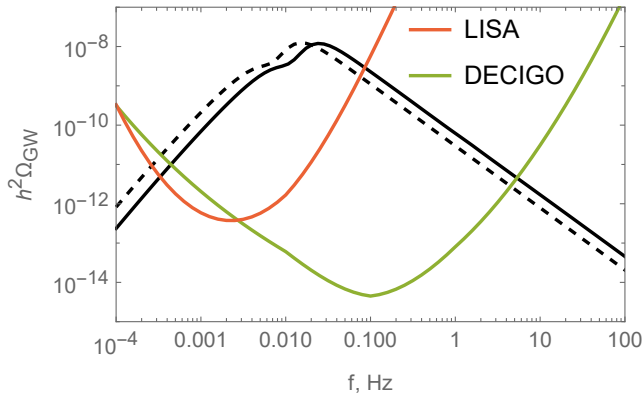


Figure 8: The GW background predicted by the model a_4 with the parameter choice (49) (the solid black curve), and by the model b_3 with the parameter choice (53) (the dashed curve).

signature of PBH, being complementary to another primordial GW signal induced by PBH Poisson fluctuations in Starobinsky gravity [46] and VAS supergravity, see Ref. [47] also.

The canonical inflaton and axion masses, and the SUSY breaking parameters in our two examples are given in Table 4. There is a small difference in the mass values, while the SUSY breaking scale is slightly higher in the b_3 model. The axion mass is higher than the inflaton mass in both cases,⁷ while inflaton can be lighter or heavier than gravitino depending upon the model. Since a precise location of the peak varies within the available window in Fig. 7, the masses in Table 4 slightly vary as well.

	m_φ/GeV	m_τ/GeV	$\langle m_{3/2} \rangle/\text{GeV}$	$\langle F^S \rangle/\text{GeV}^2$	$\langle F^T \rangle/\text{GeV}^2$
Model a_4	1.07×10^{14}	1.22×10^{14}	1.97×10^{13}	7.82×10^{31}	1.11×10^{32}
Model b_3	5.05×10^{13}	3.30×10^{14}	6.87×10^{13}	2.75×10^{32}	1.99×10^{32}

Table 4: The canonical masses of inflaton φ and axion (sinflaton) τ , the gravitino mass, and the SUSY breaking F-field VEV in our two PBH-as-whole-DM models described in this Section.

5 Conclusion

In this work we studied PBH production from (effectively) single-field ultra-slow-roll phase in the framework of Volkov–Akulov–Starobinsky supergravity, which combines non-linearly realized spontaneously broken $N = 1$ supersymmetry and Starobinsky inflation. The VAS supergravity is based on the no-scale Kähler potential (3) including the inflaton chiral superfield T and the nilpotent superfield S , and the bilinear superpotential [11, 12]. In order to introduce a near-inflection point to the scalar potential for ultra-slow-roll phase, we generalize the superpotential to a general polynomial of the form (6) without changing the Kähler potential. We

⁶When $f_{\text{tot}} = 1$, this parameter choice is just an example that is not unique.

⁷We find that the effective axion mass at the horizon exit is 6.92×10^{13} GeV and 7.04×10^{13} GeV in the models a_4 and b_3 , respectively, while it does not significantly change during the whole inflation. This means that the axion is stabilized throughout the inflationary history. It is to be compared to the Hubble function value at the horizon exit, which is $H_* = 3.49 \times 10^{13}$ GeV and $H_* = 3.55 \times 10^{13}$ GeV in the models a_4 and b_3 , respectively.

find that the superpotential must include at least a quartic term, either $W \supset T^4$ or $W \supset ST^3$, in order to support an inflection point. We give the specific examples for each quartic term, where PBH describe whole dark matter.

Our approach offers several advantages over the other Starobinsky-like PBH-DM models known in the literature. First, spontaneous SUSY breaking is automatically included by imposing the nilpotency constraint on S . It makes the effective low-energy field theory blind to the ultra-violet (UV) dynamics that gives rise to the nilpotency constraint. Second, flexibility of our model (given by its superpotential) allows us to keep the inflationary observables n_s and r within the current CMB bounds (at the 1σ confidence level), while producing the whole PBH-DM in the observationally allowed asteroid-mass window. Our models predict potentially observable gravitational waves (GW) from two different origins: (i) primordial GW leading to a relatively large tensor-to-scalar ratio r , which could be tested by more precise CMB measurements such as LiteBIRD project [48] in the future, and (ii) large scalar-induced GW that could be tested by the space-based GW interferometers such as LISA [42] and DECIGO [43].

Another relevant phenomenological aspect of our models is spontaneous SUSY breaking whose scale is directly related to the scale of inflation, around $10^{13} - 10^{14}$ GeV.

Acknowledgements

YA was supported by Thailand NSRF via the Program Management Unit for Human Resources and Institutional Development, Research and Innovation, under the grant Nos. B01F650006 and B05F650021. SVK was supported by the World Premier International Research Center Initiative (WPI Initiative), MEXT, Japan, the Japanese Society for Promotion of Science under the grant No. 22K03624, and the Tomsk Polytechnic University Development Program Priority-2030-NIP/EB-004-0000-2022.

The authors thank Sayantan Choudhury, Guillem Domenech, Jinsu Kim, Florian Kuhnel and Theodoros Papanikolaou for discussions and correspondence.

Appendix: Mukhanov-Sasaki equation

The Mukhanov-Sasaki (MS) equation [39, 40] describes the evolution of scalar perturbations,

$$\left(\frac{d^2}{d\tau^2} + k^2 - \frac{d^2 z}{z d\tau^2} \right) u_k = 0 , \quad (55)$$

where τ is conformal time ($d\tau = dt/a$), $z \equiv \frac{d\phi}{H d\tau}$, and $u \equiv z\mathcal{R}$ (u_k is its k -mode), for a comoving curvature perturbation \mathcal{R} .

It is convenient to rewrite the MS equation in terms of the e-folds variable N , see e.g., Refs. [49, 50]. Here we use the MS equation in the form

$$u_k'' + (1 - \epsilon)u_k + \left[\frac{k^2}{(aH)^2} + (1 + \frac{1}{2}\eta)(\epsilon - \frac{1}{2}\eta - 2) - \frac{1}{2}\eta' \right] u_k = 0 , \quad (56)$$

with the definitions of the slow-roll parameters as $\epsilon \equiv -H'/H$ and $\eta \equiv \epsilon'/\epsilon$. The $u_k(N)$ begins to evolve deep inside the horizon, when $k \gg aH$, with the Bunch-Davies initial condition

$$u_k = \frac{e^{-ik\tau}}{\sqrt{2k}} , \quad (57)$$

where conformal time is related to N as $d\tau = dN/(aH)$. The solution $u_k(N)$ for each mode k is used to build the power spectrum of scalar perturbations,

$$P_{\mathcal{R}} = \frac{k^3}{2\pi^2} \left| \frac{u_k}{z} \right|_{k \ll aH}^2, \quad (58)$$

to be evaluated at a later time when $k \ll aH$, in order to allow the mode u_k to stabilize at a constant value.

References

- [1] M. Rocek, “Linearizing the Volkov-Akulov Model,” *Phys. Rev. Lett.* **41** (1978) 451–453.
- [2] E. A. Ivanov and A. A. Kapustnikov, “General Relationship Between Linear and Nonlinear Realizations of Supersymmetry,” *J. Phys. A* **11** (1978) 2375–2384.
- [3] U. Lindstrom and M. Rocek, “Constrained local superfields,” *Phys. Rev. D* **19** (1979) 2300–2303.
- [4] E. A. Ivanov and A. A. Kapustnikov, “The nonlinear realization structure of models with spontaneously broken supersymmetry,” *J. Phys. G* **8** (1982) 167–191.
- [5] S. Samuel and J. Wess, “A Superfield Formulation of the Nonlinear Realization of Supersymmetry and Its Coupling to Supergravity,” *Nucl. Phys. B* **221** (1983) 153–177.
- [6] R. Casalbuoni, S. De Curtis, D. Dominici, F. Feruglio, and R. Gatto, “Nonlinear Realization of Supersymmetry Algebra From Supersymmetric Constraint,” *Phys. Lett. B* **220** (1989) 569–575.
- [7] T. Hatanaka and S. V. Ketov, “On the universality of Goldstino action,” *Phys. Lett. B* **580** (2004) 265–272, [arXiv:hep-th/0310152](#).
- [8] Z. Komargodski and N. Seiberg, “From Linear SUSY to Constrained Superfields,” *JHEP* **09** (2009) 066, [arXiv:0907.2441 \[hep-th\]](#).
- [9] S. M. Kuzenko and S. J. Tyler, “Relating the Komargodski-Seiberg and Akulov-Volkov actions: Exact nonlinear field redefinition,” *Phys. Lett. B* **698** (2011) 319–322, [arXiv:1009.3298 \[hep-th\]](#).
- [10] D. V. Volkov and V. P. Akulov, “Is the Neutrino a Goldstone Particle?,” *Phys. Lett.* **46B** (1973) 109–110.
- [11] I. Antoniadis, E. Dudas, S. Ferrara, and A. Sagnotti, “The Volkov–Akulov–Starobinsky supergravity,” *Phys. Lett. B* **733** (2014) 32–35, [arXiv:1403.3269 \[hep-th\]](#).
- [12] Y. Aldabergenov, “Volkov–Akulov–Starobinsky supergravity revisited,” *Eur. Phys. J. C* **80** no. 4, (2020) 329, [arXiv:2001.06617 \[hep-th\]](#).
- [13] G. Dall’Agata and F. Zwirner, “On goldstino-less supergravity models of inflation,” *JHEP* **12** (2014) 172, [arXiv:1411.2605 \[hep-th\]](#).
- [14] G. Domènech, “Scalar Induced Gravitational Waves Review,” *Universe* **7** no. 11, (2021) 398, [arXiv:2109.01398 \[gr-qc\]](#).

- [15] A. Escrivà, F. Kuhnel, and Y. Tada, “Primordial Black Holes,” [arXiv:2211.05767 \[astro-ph.CO\]](#).
- [16] I. Dalianis, A. Kehagias, and G. Tringas, “Primordial black holes from α -attractors,” *JCAP* **01** (2019) 037, [arXiv:1805.09483 \[astro-ph.CO\]](#).
- [17] R. Mahbub, “Primordial black hole formation in inflationary α -attractor models,” *Phys. Rev. D* **101** no. 2, (2020) 023533, [arXiv:1910.10602 \[astro-ph.CO\]](#).
- [18] Y. Aldabergenov, A. Addazi, and S. V. Ketov, “Primordial black holes from modified supergravity,” *Eur. Phys. J. C* **80** no. 10, (2020) 917, [arXiv:2006.16641 \[hep-th\]](#).
- [19] D. V. Nanopoulos, V. C. Spanos, and I. D. Stamou, “Primordial Black Holes from No-Scale Supergravity,” *Phys. Rev. D* **102** no. 8, (2020) 083536, [arXiv:2008.01457 \[astro-ph.CO\]](#).
- [20] S. V. Ketov, “Multi-Field versus Single-Field in the Supergravity Models of Inflation and Primordial Black Holes,” *Universe* **7** no. 5, (2021) 115.
- [21] Y. Aldabergenov, A. Addazi, and S. V. Ketov, “Inflation, SUSY breaking, and primordial black holes in modified supergravity coupled to chiral matter,” *Eur. Phys. J. C* **82** no. 8, (2022) 681, [arXiv:2206.02601 \[astro-ph.CO\]](#).
- [22] D. Frolovsky, S. V. Ketov, and S. Saburov, “E-models of inflation and primordial black holes,” *Front. in Phys.* **10** (2022) 1005333, [arXiv:2207.11878 \[astro-ph.CO\]](#).
- [23] M. Braglia, A. Linde, R. Kallosh, and F. Finelli, “Hybrid α -attractors, primordial black holes and gravitational wave backgrounds,” [arXiv:2211.14262 \[astro-ph.CO\]](#).
- [24] J. Garcia-Bellido and E. Ruiz Morales, “Primordial black holes from single field models of inflation,” *Phys. Dark Univ.* **18** (2017) 47–54, [arXiv:1702.03901 \[astro-ph.CO\]](#).
- [25] C. Germani and T. Prokopec, “On primordial black holes from an inflection point,” *Phys. Dark Univ.* **18** (2017) 6–10, [arXiv:1706.04226 \[astro-ph.CO\]](#).
- [26] V. De Luca and A. Riotto, “A note on the abundance of primordial black holes: Use and misuse of the metric curvature perturbation,” *Phys. Lett. B* **828** (2022) 137035, [arXiv:2201.09008 \[astro-ph.CO\]](#).
- [27] A. Riotto, “The Primordial Black Hole Formation from Single-Field Inflation is Not Ruled Out,” [arXiv:2301.00599 \[astro-ph.CO\]](#).
- [28] S. Choudhury, M. R. Gangopadhyay, and M. Sami, “No-go for the formation of heavy mass Primordial Black Holes in Single Field Inflation,” [arXiv:2301.10000 \[astro-ph.CO\]](#).
- [29] H. Motohashi and W. Hu, “Primordial Black Holes and Slow-Roll Violation,” *Phys. Rev. D* **96** no. 6, (2017) 063503, [arXiv:1706.06784 \[astro-ph.CO\]](#).
- [30] A. A. Starobinsky, “A new type of isotropic cosmological models without singularity,” *Phys. Lett. B* **91** no. 1, (1980) 99 – 102.

- [31] V. R. Ivanov, S. V. Ketov, E. O. Pozdeeva, and S. Y. Vernov, “Analytic extensions of Starobinsky model of inflation,” *JCAP* **03** no. 03, (2022) 058, [arXiv:2111.09058 \[gr-qc\]](#).
- [32] **BICEP, Keck** Collaboration, P. A. R. Ade *et al.*, “Improved Constraints on Primordial Gravitational Waves using Planck, WMAP, and BICEP/Keck Observations through the 2018 Observing Season,” *Phys. Rev. Lett.* **127** no. 15, (2021) 151301, [arXiv:2110.00483 \[astro-ph.CO\]](#).
- [33] M. Tristram *et al.*, “Improved limits on the tensor-to-scalar ratio using BICEP and Planck data,” *Phys. Rev. D* **105** no. 8, (2022) 083524, [arXiv:2112.07961 \[astro-ph.CO\]](#).
- [34] W. H. Press and P. Schechter, “Formation of galaxies and clusters of galaxies by selfsimilar gravitational condensation,” *Astrophys. J.* **187** (1974) 425–438.
- [35] K. Inomata, M. Kawasaki, K. Mukaida, Y. Tada, and T. T. Yanagida, “Inflationary Primordial Black Holes as All Dark Matter,” *Phys. Rev. D* **96** no. 4, (2017) 043504, [arXiv:1701.02544 \[astro-ph.CO\]](#).
- [36] K. Inomata, M. Kawasaki, K. Mukaida, and T. T. Yanagida, “Double inflation as a single origin of primordial black holes for all dark matter and LIGO observations,” *Phys. Rev. D* **97** no. 4, (2018) 043514, [arXiv:1711.06129 \[astro-ph.CO\]](#).
- [37] B. J. Carr, “The Primordial black hole mass spectrum,” *Astrophys. J.* **201** (1975) 1–19.
- [38] I. Musco, “Threshold for primordial black holes: Dependence on the shape of the cosmological perturbations,” *Phys. Rev. D* **100** no. 12, (2019) 123524, [arXiv:1809.02127 \[gr-qc\]](#).
- [39] V. F. Mukhanov, “Gravitational Instability of the Universe Filled with a Scalar Field,” *JETP Lett.* **41** (1985) 493–496.
- [40] M. Sasaki, “Large Scale Quantum Fluctuations in the Inflationary Universe,” *Prog. Theor. Phys.* **76** (1986) 1036.
- [41] B. Carr, K. Kohri, Y. Sendouda, and J. Yokoyama, “Constraints on primordial black holes,” *Rept. Prog. Phys.* **84** no. 11, (2021) 116902, [arXiv:2002.12778 \[astro-ph.CO\]](#).
- [42] **LISA** Collaboration, P. Amaro-Seoane *et al.*, “Laser Interferometer Space Antenna,” [arXiv:1702.00786 \[astro-ph.IM\]](#).
- [43] H. Kudoh, A. Taruya, T. Hiramatsu, and Y. Himemoto, “Detecting a gravitational-wave background with next-generation space interferometers,” *Phys. Rev. D* **73** (2006) 064006, [arXiv:gr-qc/0511145](#).
- [44] J. R. Espinosa, D. Racco, and A. Riotto, “A Cosmological Signature of the SM Higgs Instability: Gravitational Waves,” *JCAP* **09** (2018) 012, [arXiv:1804.07732 \[hep-ph\]](#).
- [45] N. Bartolo, V. De Luca, G. Franciolini, A. Lewis, M. Peloso, and A. Riotto, “Primordial Black Hole Dark Matter: LISA Serendipity,” *Phys. Rev. Lett.* **122** no. 21, (2019) 211301, [arXiv:1810.12218 \[astro-ph.CO\]](#).

- [46] T. Papanikolaou, C. Tzerefos, S. Basilakos, and E. N. Saridakis, “Scalar induced gravitational waves from primordial black hole Poisson fluctuations in $f(R)$ gravity,” *JCAP* **10** (2022) 013, [arXiv:2112.15059](#) [[astro-ph.CO](#)].
- [47] S. Kawai and J. Kim, “Primordial black holes and gravitational waves from nonminimally coupled supergravity inflation,” [arXiv:2209.15343](#) [[astro-ph.CO](#)].
- [48] **LiteBIRD** Collaboration, E. Allys *et al.*, “Probing Cosmic Inflation with the LiteBIRD Cosmic Microwave Background Polarization Survey,” [arXiv:2202.02773](#) [[astro-ph.IM](#)].
- [49] G. Ballesteros and M. Taoso, “Primordial black hole dark matter from single field inflation,” *Phys. Rev. D* **97** no. 2, (2018) 023501, [arXiv:1709.05565](#) [[hep-ph](#)].
- [50] S. V. Ketov, E. O. Pozdeeva, and S. Y. Vernov, “On the superstring-inspired quantum correction to the Starobinsky model of inflation,” *JCAP* **12** (2022) 032, [arXiv:2211.01546](#) [[gr-qc](#)].